

Lipid Vesicle Fusion on μ CP Patterned Self-Assembled Monolayers: Effect of Pattern Geometry on Bilayer Formation

A. Toby A. Jenkins,^{*,†} Richard J. Bushby,[‡] Stephen D. Evans,[‡] Wolfgang Knoll,[§] Andreas Offenhäusser,[‡] and Simon D. Ogier^{‡,¶}

Department of Chemistry, University of Bath, Bath, BA2 7AY U.K., Centre for Self-Organising Molecular Systems, University of Leeds, Leeds, LS2 9JT, UK, Max-Planck-Institut für Polymerforschung, Ackermannweg 10, 55128 Mainz, Germany, and Forschungszentrum Jülich, 52425 Jülich, Germany

Received October 3, 2001. In Final Form: January 14, 2002

Microcontact printing (μ CP) of lipophilic self-assembled monolayers (SAMs) has been used to fabricate micron dimensioned patterned surfaces that can be used as a means of attaching lipid bilayers to solid surfaces. This communication addresses how variation in the patterned SAM geometry affects vesicle adsorption. The substrates consisted of circular hydrophilic regions functionalized with mercaptoethanol surrounded by octadecanethiol (ODT). Three geometries were studied in which the diameter of the hydrophilic portion was varied between 4 and 16 μ m and the center-to-center separation was varied between 10 and 40 μ m. Thus, it was possible to study lipid adsorption on SAM systems with the same total hydrophilic surface area, but with different sized hydrophilic patches. Impedance spectroscopy showed that for the films of the same total hydrophilic area greater lipid coverage was obtained for SAMs with smaller diameter hydrophilic patches. To understand this observation, tapping mode AFM and surface plasmon microscopy were used to study lipid vesicles adsorption on such surfaces. A new mode of vesicle adsorption on micropatterned hydrophobic/hydrophilic surfaces is presented which shows that the simple picture of a bilayer spanning the hydrophilic patches is overly simplistic and that the real situation is considerably more complex and that the hydrophobic–hydrophilic edge plays an important role.

Introduction

The plasma membrane exists within cells to control the flow of ions, metabolites, etc., between the extra- and intracellular regions. This important function is achieved by the incorporation of membrane spanning proteins and peptides. The mode of action of these varies. Many form an ion channel through the membrane on application of an external trigger, such as potential change (voltage gating) or analyte interaction (ligand gating). The ultimate aim of the work presented here is to utilize this effect by creating a biomimetic membrane on a solid surface. Such surfaces would be of interest for two reasons: First, they would form the basis for the next generation of biosensors, utilizing Nature's own biosensing mechanisms, and second, they would provide ideal systems for cell membrane protein structure–function studies. A number of researchers have effectively reviewed this area in recent years, especially Sackmann and Groves.^{1,2}

The micropatterning of solid substrates with self-assembled monolayers (SAMs) has been shown to be an effective way of producing an array of functionally active bilayer patches on a surface.^{3,4} The use of micropatterning

provides a high degree of control of the spatial distribution of lipophilic support molecules, in this case octadecanethiol (ODT). The remaining surface is then functionalized with a hydrophilic moiety mercaptoethanol.

During vesicle adsorption it is believed that a lipid monolayer is adsorbed at hydrophobic surfaces while a “true” lipid bilayer is adsorbed on the hydrophilic regions. Furthermore, studies have shown that membrane proteins will self-locate into such “bilayer patches”, where the lipids are mobile.⁵

Figure 1 presents schematically the view generally presented in the literature for vesicle interactions with nonpatterned hydrophobic (a) and hydrophilic surfaces (b).⁶ This paper is concerned with understanding the nature of lipid adsorption at micropatterned SAMs. In particular, we are interested in the hydrophilic regions, where the driving force for bilayer formation vs unruptured vesicle adsorption may be weak.

Measurements presented in this paper show that lipid adsorption in the hydrophilic, mercaptoethanol SAM regions is far from simple. To understand this properly requires consideration of the edge effects at the interface between the hydrophobic and hydrophilic regions as well as vesicle interaction with hydrophilic surfaces.^{3,4,7} The experimental results presented here suggest that on relatively large hydrophilic patches, some of the adsorbed lipid may not be unrolled but be sitting on the mercaptoethanol surface as lipid vesicles. The evidence for comes

[†] University of Bath.

[‡] University of Leeds.

[§] Max-Planck-Institut für Polymerforschung.

[‡] Forschungszentrum Jülich.

[¶] Present address: Avecia, PO Box 42, Manchester M8 8ZS U.K.

* Corresponding author: e-mail a.t.a.jenkins@bath.ac.uk.

(1) Sackmann, E. *Science* **1996**, 271, 43–48.

(2) Groves, J. T.; Ulman, N.; Boxer, S. G. *Science* **1997**, 275, 651–653.

(3) Jenkins, A. T. A.; Bushby, R. J.; Boden, N.; Evans, S. D.; Knowles, P. F.; Miles, R. E.; Ogier, S. D. *Langmuir* **1998**, 14, 4675–4678.

(4) Jenkins, A. T. A.; Bushby, R. J.; Boden, N.; Evans, S. D.; Knowles, P. F.; Miles, R. E.; Ogier, S. D.; Schönherr, H.; Vancso, G. J. *J. Am. Chem. Soc.* **1999**, 121, 5274.

(5) Groves, J. T.; Ulman, N.; Boxer, S. G. *Science* **1997**, 275, 651–653. Groves, J. T.; Wulffing, C.; Boxer, S. G. *Biophys. J.* **1996**, 71, 2716–2723.

(6) Lingler, S.; Rubinstein, I.; Knoll, W.; Offenhäusser, A. *Langmuir* **1997**, 13, 7085–7091.

(7) Rädler, J.; Strey, H.; Sackmann, E. *Langmuir* **1995**, 11, 4539–4538.

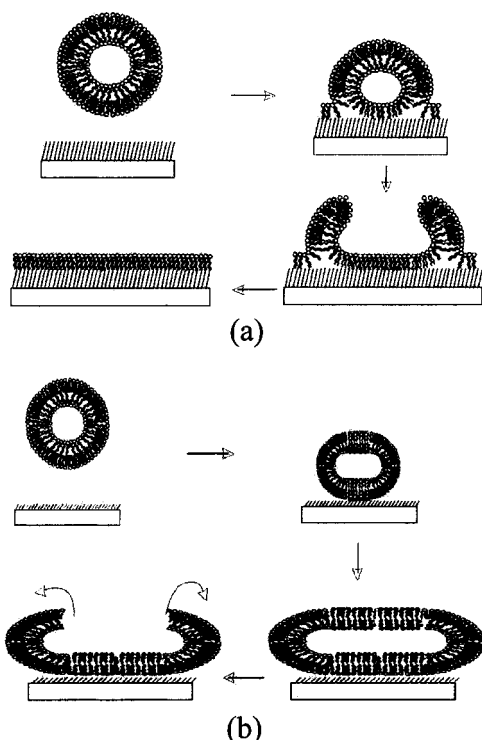


Figure 1. Schematic of conventional view of the mechanism of vesicle adsorption on (a) hydrophobic and (b) hydrophilic surfaces.

from surface plasmon resonance (SPR) and surface plasmon microscopy (SPM), impedance, and AFM measurements on micropatterned SAMs.

Previously, we have carried out studies on large ($20 \times 20 \mu\text{m}$) square-shaped hydrophilic regions (mercaptoethanol), situated $200 \mu\text{m}$ apart. The intervening region consisted of cholesterylpolyethylenoxythiol (CPEO3).⁸ This resulted in a rather small proportion of the total surface being covered with the free lipid bilayer (0.5%).^{3,4} For the present studies a photolithographic mask was designed that allowed control over the size of the hydrophilic regions and their separation, i.e., determining the ratio of hydrophobic to hydrophilic areas. Moreover, a much larger proportion of the surface (14.4%) contains hydrophilic SAM over which lipid bilayer is formed.

Electrochemical impedance spectroscopy was used to follow the electrical properties of the patterned SAMs during lipid vesicle adsorption. Impedance measurements were used to determine the capacitance of the adsorbed film.⁶ The capacitance value is strongly related to the surface coverage—even small defects and pinholes cause a large increase in the measured capacitance. Theoretically, a capacitance of around $0.45 \mu\text{F cm}^{-2}$ is expected for an ideal bilayer—SAM system of the type being described here.^{3,9,19} The capacitance change with time provides

Table 1. Pattern Dimensions of μ CP SAMs

circle diameter/ μm	intercircle spacing (center-center)/ μm	circle % area of total
4	10	14.4
8	20	14.4
16	40	14.4

information about the kinetics of the adsorption process. The resistance of the interface can also be determined by impedance spectroscopy which can then be used to obtain a value that is related to the bilayer resistance.^{3,4} In addition, SPR measurements have been used to follow the kinetics of vesicle adsorption on homogeneous single-component ODT and mercaptoethanol SAMs.

Tapping mode AFM allows one to image soft material on a surface without causing damage from the AFM tip. By using very low contact forces (down to 200 pN), it is possible to image vesicles on a surface. In this paper, we present tapping mode AFM images of lipid vesicles adsorbed on hydrophilic patches on micropatterned SAMs.

Experimental Section

Electrode and Material Preparation. For impedance measurements 120 nm of gold was thermally evaporated onto a 5 nm chromium adhesion on cleaned glass microscope slides (2% Helmanex, sonication, ethanol). For surface plasmon resonance, 50 nm of gold was evaporated directly onto cleaned high refractive index prisms ($n = 1.845$).

AFM substrates were made by evaporating 120 nm gold onto prebaked (600°C , argon, 30 s), freshly cleaved mica and then annealing at 650°C for 1 min in a tube furnace, under a flow of nitrogen. All depositions were carried out using a Balzers thermal evaporator and evaporation made at pressures $< 4 \times 10^{-6} \text{ mbar}$. Prior to microcontact printing, the gold substrates were either cleaned in ethanol (for SPR or AFM) or immersed in piranha solution ($30\% \text{ H}_2\text{O}_2/70\% \text{ H}_2\text{SO}_4$) for 1 min for other impedance measurements (caution: solution hot and highly oxidizing).

Stamp Construction. To create elastomeric stamps of the desired geometry, the following procedure was used: A chromium—glass photolithographic mask was constructed using electron beam lithography at the Rutherford-Appleton Laboratory, Oxfordshire, U.K. The mask consists of three separate patterns, each consisting of an array of circles spaced on a regular square lattice. These pattern dimensions are listed in Table 1.

The mask was used to create arrays of raised columns in SU8 photoresist (Chestech, Rugby, UK) using standard lithographic techniques. For a detailed description of microcontact printing see ref 10 and the references therein. Poly(dimethylsiloxane) (PDMS) was applied to the patterned photoresist and baked at 60°C for 1 h . The baked PDMS was subsequently peeled off and examined under an optical microscope to ensure the pattern had been effectively reproduced in the stamp. Each individual patterned stamp has gross dimensions of $7 \times 7 \text{ mm}$.

Microcontact Printing. The PDMS stamps were “inked” with 5 mM ODT solution in ethanol for 1 min , dried under a stream of nitrogen for ca. 30 s , and applied to a clean gold substrate. A higher concentration of thiol solution was used in an attempt to produce a more homogeneous SAM.^{11a,b} The stamp was left on the gold substrate for 1 min to allow time for transfer. Following transfer, the stamps were carefully peeled off; the substrate was rinsed in ethanol and then immersed for 2 min in 5 mM mercaptoethanol solution in ethanol and then rinsed in copious quantities of ethanol.

(8) Boden, N.; Bushby, R. J.; Clarkson, S.; Evans, S. D.; Knowles, P. F.; Marsh, A. *Tetrahedron* **1997**, *53*, 10939–10952.

(9) Cornell, B. A.; Braach-Maksvytis, V. L. B.; King, L. G.; Osman, P. D. J.; Raguse, B.; Wiczorek, L.; Pace, R. J. *Nature (London)* **1997**, *387*, 580–583.

(10) Xia, Y.; Whitesides, G. M. *Angew. Chem., Int. Ed.* **1998**, *37*, 4000–4025.

(11) (a) Libiouille, L.; Bietsch, A.; Schmid, H.; Michel, B.; Delamarche, E. *Langmuir* **1999**, *15*, 300–304. (b) Larsen, N. B.; Biebuyck, H.; Delamarche, E.; Michel, B. *J. Am. Chem. Soc.* **1997**, *119*, 3017–2026.

(12) Lipid Products, Nuffield, Surrey, U.K.

(13) Kalb, E.; Frey, S.; Tamm, L. K. *Biochim. Biophys. Acta* **1992**, *1103*, 307–316.

(14) Scheller, A. Winspall SPR fitting program, v. 2.01, Max-Planck-Institut für Polymerforschung, 2000.

(15) Jenkins, A. T. A.; Neumann, T.; Offenhäuser, A. *Langmuir* **2001**, *17*, 265–267.

(16) Boussaad, S.; Tao, N. J. *J. Am. Chem. Soc.* **1999**, *121*, 4510–4515.

(17) Dufrène, Y. F.; Barger, W. R.; Green, J.-B. D.; Lee, G. U. *Langmuir* **1997**, *13*, 4779–4784.

(18) Möller, C.; Allen, M.; Elings, V.; Engel, A. Müller, D. J. *Biophys. J.* **1999**, *77*, 1150.

(19) Glazier, S. A.; Vanderah, D. J.; Plant, A. L.; Bayley, H.; Valincius, G.; Kasianowicz, J. J. *Langmuir* **2000**, *16*, 10428–10435.

Lipid vesicles were prepared by hydrating egg-phosphatidylcholine (egg-PC)¹² in 0.1 M KCl for 1 h and then extruding through 50 nm diameter polycarbonate membranes for 18 cycles at a concentration of 1 mg/mL. The resultant vesicle size will be between 60 and 70 nm.¹³ Vesicles were subsequently diluted to 0.2 mg/mL in further 0.1 M KCl.

Measurements. SPR and impedance measurements were not performed simultaneously because previous experiments have shown that impedance is very sensitive to gold roughness and pretreatment.³ It was found that the thinner SPR gold substrates have poorer electrical characteristics (in terms of the resistance and capacitance of self-assembled monolayers adsorbed thereon) than the 120 nm of gold on a chromium adhesion layer used for electrochemistry. A small pinhole defect in an adsorbed film has a large effect on the measured impedance, while a small defect on an SPR prepared substrate is generally not "seen" by SPR.

Electrochemical impedance measurements were made on a Solartron 1260 frequency response analyzer together with an EG&G PAR 273A potentiostat. The cell was operated in a two-electrode mode, with a coiled platinum wire counter electrode. A 12 mV rms ac potential was applied at the open-circuit potential of the cell. The applied ac frequency was swept between 50 kHz and 300 mHz. Measurements were first made on the bare SAM in 0.1 M KCl, and then measurements were made at regular intervals during lipid adsorption; subsequently, the cell was then rinsed and a final measurement made.³ A discussion of the fitting and interpretation of impedance results is given later.

SPR measurements were using a system described previously by Lingler et al.⁶ SPR measurements were made on homogeneous, liquid formed ODT and mercaptoethanol (e01) SAMs. The adsorbed lipid film thickness was thus determined by measuring first the SAM system under fluid (0.1 M KCl), then adsorbing lipid vesicles, rinsing after adsorption (Figure 4), and measuring another SPR curve. The SPR curves of the SAM was fitted using an iterative fitting program based on the Fresnel equations, allowing the gold optical properties and thickness to vary slightly to give best fit.¹⁴ The adsorbed lipid thickness was calculated by fixing the SAM/gold variables and adding a new layer in the fitting procedure pertaining to the adsorbed lipid.

The SPR instrument was subsequently converted to a surface plasmon microscope by the relatively simple procedure of adding a spatial filter to the optical track before the sample (to give a broad laser illumination) and incorporating a zoom objective and CCD camera in place of the photodiode. Measurements of lipid adsorption on the homogeneous SAMs and micropatterned SAMs are given in Figure 4. The thickness measurements obtained for the micropatterned SAMs were not obtained by fitting the angular dependent SPR curves to a Fresnel model, but instead the measured gray scale at a fixed angle was converted to a film thickness value. The thickness of lipid on the μ CP ODT layer was used to convert the gray scale data to thickness. The gray scale value at $t = 0$ was set to 0 Å adsorbed lipid, on both the μ CP ODT and μ CP mercaptoethanol areas. The thickness of the lipid adsorbed on the 100% ODT SAM was determined by Fresnel fitting to be 18 Å. As a result, the change in gray scale from $t = 0$ to after vesicle adsorption and rinsing on the μ CP ODT was also equated to a thickness of 18 Å. The gray scale could thus be converted to film thickness, so allowing the thickness of lipid adsorbed in the mercaptoethanol areas to be calculated. Further experimental details and a comprehensive treatment of the results are given in ref 15.

AFM measurements were made on a Nanoscope IIIa AFM in tapping mode. Contact force was around 0.12 N m⁻¹ and tapping frequency between 10 and 30 kHz. Measurements were made under 0.1 M KCl electrolyte, after 1 h of vesicle adsorption on the patterned SAM.

Results and Discussion

Impedance Measurements. a. Fitting and Interpretation of Impedance Results. In general, only one time constant was observed for the systems shown here. That is, the spectra display just one feature, and further deconvolution of the spectra is not possible. The high frequency part of the spectra is generally accepted to pertain to the impedance of the organic film while the low

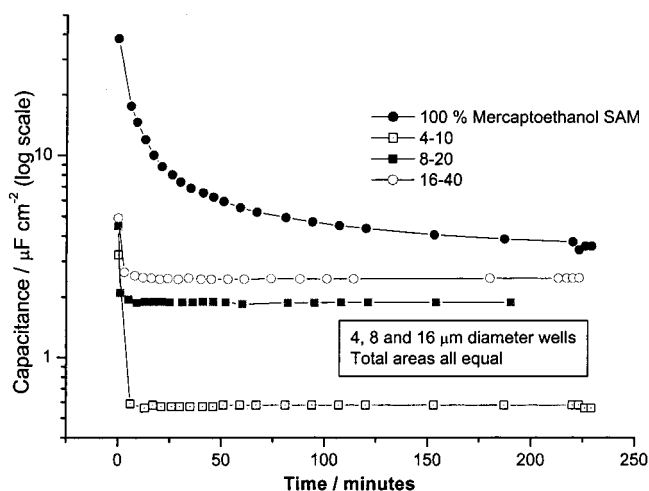


Figure 2. Change in capacitance of the SAM–lipid system as extruded egg-PC lipid vesicles adsorbing on the μ CP SAMs.

frequency, purely capacitive, impedance can be ascribed to the gold double-layer capacitance. Therefore, by fitting a simple RC series circuit to the data in the range 50 kHz–1 kHz, it is reasonable to approximate the capacitance of the organic film. This can be clearly observed if impedance data are plotted as admittance divided by frequency, i.e., y'/ω vs y''/ω . A semicircle relating to the film capacitance was clearly observed. This fitting procedure has been described in a previous communication by Lingler et al. and Jenkins et al.^{3,6}

b. Comparison of Vesicle Adsorption on Different μ CP SAMs. The stamp design allows for the comparison of micropatterned ODT SAMs, all with different pattern geometries, but with identical total areas of hydrophobic ODT and hydrophilic mercaptoethanol. In addition, for comparison, the adsorption of lipid vesicles on a pure mercaptoethanol SAM is shown. As discussed in some detail in a previous communication, the coverage of lipid on a patterned SAM is inversely related to its capacitance.⁴ Therefore, measuring the change in capacitance, as lipid vesicles adsorb on the three micropatterned systems, it is possible to infer information about the relative degree of bilayer coverage on the hydrophilic wells.

Figure 2 shows the change in capacitance on the 4–10 (4 μ m diameter wells, 10 μ m apart), 8–20, and 16–40 systems. It is clear that the patterned SAMs with smaller diameter hydrophilic wells have lower capacitances (and so greater bilayer coverage) after ca. 100 min adsorption, despite the total hydrophilic area of all the SAMs being identical. The adsorption of lipid on a pure 100% mercaptoethanol SAM is given for comparison. This trend was seen many times, including on micropatterned thiolethoxy cholesterol (CPEO3)–mercaptoethanol SAM systems.⁴

To understand these results, two further experiments using atomic force microscopy (AFM) and surface plasmon microscopy were performed in order to attempt to better observe what happens when vesicles adsorb on micropatterned surfaces. The results of the surface plasmon microscopy measurements have been already published as a short communication but are partly included here as they help to explain the observed experimental results.

c. AFM Measurements. AFM measurements were performed in tapping mode.^{16,17} Tapping permits imaging with much reduced forces between the tip and the substrate. This allows imaging of fragile substances only weakly bound to the surface, such as proteins or lipids, without destroying them.¹⁸ Tapping mode measurements

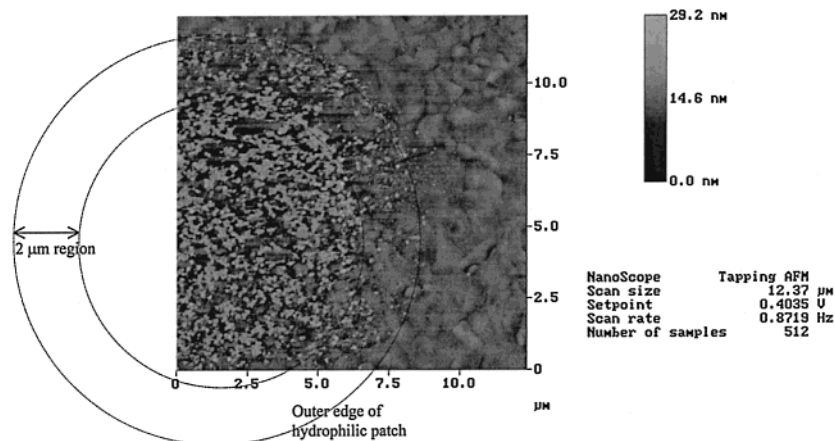


Figure 3. Tapping mode AFM image of adsorbed lipid on μ CP stamped 16–40 SAM. Note adsorption of vesicles (white spots) in hydrophilic well and well edge region of approximately 2 μ m width.

made after 90 min lipid adsorption in 0.1 M KCl on the μ CP SAMs are interesting. Figure 3 shows the intersection between a hydrophilic region (lower left corner) and its hydrophobic surroundings. On the hydrophilic region one can see small, ca. 100 nm, diameter particles that we assume (because of their thickness) are fused vesicles, adsorbed on the surface. However, these are not seen on the hydrophobic surroundings. Importantly, there is a region that extends approximately 2 μ m into the hydrophilic SAM (from the hydrophobic SAM edge) in which the number of adsorbed vesicles appears to be diminished, and we assume lipid bilayer is present. This region is marked in Figure 3. Cross-section analysis of one of the particles gave a height of ca. 11 nm—approximately the height of a “squashed” vesicle.

The fact vesicles are not seen in large numbers near the edge of the hydrophilic regions suggests that the interaction of vesicles with the hydrophobic region may be of great importance in causing the vesicles to rupture and hence in bilayer formation.

Surface Plasmon Microscopy. The patterned SAM was imaged before, during, and following vesicle adsorption. The gray scale of these images was obtained, on both the hydrophobic ODT and the mercaptoethanol filled wells, thus giving spatially and time-resolved information on the change in thickness of the SAM–lipid system as lipid vesicles adsorbed. Twelve separate areas of both hydrophobic and hydrophilic surface were measured by gray-scale analysis, and the results were averaged. As noted previously, it was assumed that a lipid monolayer was formed on the hydrophobic ODT areas. This assumption allowed quantification of the measured gray scale (vide supra).

Figure 4 shows how the thickness of lipid changes on both the hydrophobic and hydrophilic patterned regions, and as an important comparison, the conventional SPR results from nonpatterned ODT and mercaptoethanol SAMs formed from solution (not μ CP).

Lipid vesicle adsorption on the hydrophobic regions on both the liquid formed 100% ODT SAMs and the μ CP ODT areas both show similar behavior. Analysis of lipid adsorption on the hydrophilic mercaptoethanol regions of the patterned SAM and on the 100% liquid formed mercaptoethanol SAMs shows a very different effect. Lipid adsorption on the 100% mercaptoethanol SAM gave a final thickness of 85 Å, too great for a lipid bilayer, but consistent with forming a monolayer of adsorbed vesicles. The adsorption curve is of the expected Langmuir type. Lipid vesicle adsorption on the hydrophilic mercaptoethanol regions of the μ CP SAM is more complex. The final

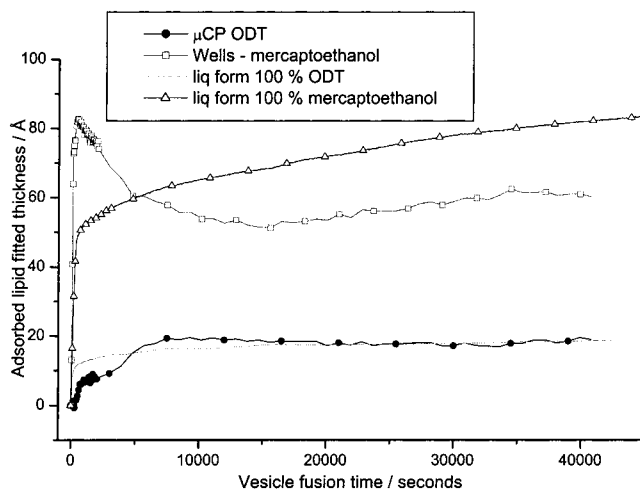


Figure 4. Kinetics of egg-PC vesicle adsorption on (i) 100% ODT SAMs and 100% mercaptoethanol SAMs with thicknesses determined by Fresnel fitting and (ii) egg-PC vesicle adsorption on micropatterned ODT and mercaptoethanol SAMs, with lipid layer thickness estimated from conversion of measured gray-scale values (from SPM measurements) to thickness values.¹⁵

thickness of 60 Å is intermediate between that of a bilayer (ca. 45 Å) and adsorbed vesicles (ca. 85 Å), suggesting that a mixture of both adsorbed vesicles and bilayer is formed, which is consistent with the AFM results shown in Figure 3. The initial increase in thickness is also at the rate found for the pure mercaptoethanol (in the first 300 s). The overall shape of the curve is more difficult to interpret but is consistent with the idea of rapid vesicle adsorption followed by rupture.

Conclusions

The impedance measurements presented here show higher coverage of lipid bilayer or reduced “leakiness” of lipid bilayer on small dimensioned hydrophilic wells compared with larger wells, despite all three systems having identical total hydrophilic areas (Figure 1). Tapping mode AFM and surface plasmon microscopy (SPM) results suggest a possible explanation for these results, and the three experiments considered together present an interesting picture of the mechanism vesicle adsorption on such patterned surfaces. We suggest here two possible models for vesicle adsorption and bilayer formation on micropatterned SAMs of the type discussed here.

When a lipid vesicle adsorbs on hydrophobic region (e.g., ODT SAM), surface energy driving forces are such that

Table 2. Comparison of Total Edge Length at Hydrophilic–Hydrophobic Interface with Capacitance of Adsorbed Lipid Film

system	total edge length/m cm ⁻²	capacitance after vesicle fusion/ μ F cm ⁻²
4–10	12.57	0.56
8–20	6.28	1.88
16–40	3.14	2.47

the vesicle rapidly “bursts” and forms a lipid monolayer, with the hydrophilic lipid headgroups uppermost on the adlayer.

When a vesicle adsorbs on a hydrophilic mercaptoethanol region, the situation is more complex. It appears from the tapping mode AFM images that vesicles in the proximity of the hydrophobic edge are present in lower number. A number of explanations are possible: One explanation is that initially vesicles adsorb evenly across the mercaptoethanol SAM, but then vesicles in the proximity of the hydrophobic edge rupture and form a ring of lipid bilayer. This suggests that the edges act as either fusogenic or nucleation sites for bilayer growth. An alternative possibility is that adsorbed vesicles have some surface mobility and by “random walk” migrate to the edges where they rupture. In either case the fact that the ODT/mercaptoethanol edge will not be sharp, but a diffuse region, will enhance both the above two mechanisms.

Impedance measurements support these models, showing less leaky bilayers on smaller diameter wells. Moreover, it would be expected for both models that systems with the greatest total edge length (that is, the total circumference of all the hydrophilic regions per unit area) would exhibit the lowest capacitance for the adsorbed lipid layer. This was indeed found, the results are summarized in Table 2:

The behavior of lipid vesicles adsorbed on hydrophilic substrates shown here correlates well with a study of lipid adsorption on rough hydrophilic surfaces made by Rädler et al., who have used reflectance interference contrast microscopy to study lipid adsorption on relatively rough MgF₂-coated glass.⁷ They found that lipid films adsorbed on such surfaces had thicknesses which varied between one and two bilayers and that coverage was not complete. These are in agreement with the observations made here on micropatterned SAMs containing hydrophilic islands surrounded by hydrophobic regions.

One of the reasons for investigating the effect of well geometry on μ CP supported lipid bilayers is to provide a more blocking lipid bilayer environment into which peptides and proteins can be inserted and their function measured. Previous measurements of the relative conductivity of the cation size selective ion channel, gramicidin, by Jenkins et al. of K⁺ and Cs⁺ ion conductance showed a 10% greater conductance of Cs⁺ compared to that of K⁺ on large (20 \times 20 μ m) patterned wells.⁴ Measurements of gramicidin activity measured on bilayer adsorbed on 4 μ m diameter mercaptoethanol wells showed, in comparison, a 300% greater conductivity of Cs⁺ to K⁺. In these systems with a more blocking lipid bilayer there is less non-ion-selective leakage, and so the selectivity of the gramicidin is more clearly revealed.

Acknowledgment. We thank R. E. Miles and P. F. Knowles (University of Leeds) for useful discussions and V. Scheumann (MPIP-Mainz) for AFM measurements. A.T.A.J. acknowledges the support of the Max-Planck-Society and the Alexander-von-Humboldt Stiftung for financing his work.

LA011510P